Nafise Naseri, Fatemeh Parastesh, Farnaz Ghassemi, Sajad Jafari, Eckehard Schöll, Jürgen Kurths

Converting high-dimensional complex networks to lower-dimensional ones preserving synchronization features

Citation details
Naseri, N., Parastesh, F., Ghassemi, F., Jafari, S., Schöll, E., & Kurths, J. (2022). Converting high-dimensional complex networks to lower-dimensional ones preserving synchronization features. In Europhysics Letters (Vol. 140, Issue 2, p. 21001). IOP Publishing. https://doi.org/10.1209/0295-5075/ac98de.

Converting high dimensional complex networks to lower dimensional ones preserving synchronization features

Nafise Naseri[1], Fatemeh Parastesh[1], Farnaz Ghassemi[1], Sajad Jafari*[1,2], Eckehard Schöll[3,4,5], Jürgen Kurths[5,6]

[1] *Department of Biomedical Engineering, Amirkabir University of Technology (Tehran polytechnic), Iran*
[2] *Health Technology Research Institute, Amirkabir University of Technology (Tehran polytechnic), Iran*
[3] *Institut für Theoretische Physik, Technische Universität Berlin, Hardenbergstrasse 36, 10623 Berlin, Germany*
[4] *Bernstein Center for Computational Neuroscience Berlin, Humboldt-Universität, 10115 Berlin, Germany*
[5] *Potsdam Institute for Climate Impact Research, Telegrafenberg A 31, 14473 Potsdam, Germany*
[6] *Humboldt University Berlin, Department of Physics, Berlin, 12489, Germany*

PACS `89.75.-k` – Complex systems
PACS `05.45.Xt` – Synchronization

Abstract –Studying the stability of synchronization of coupled oscillators is one of the prominent topics in network science. However, in most cases, the computational cost of complex network analysis is challenging because they consist of a large number of nodes. This study includes overcoming this obstacle by presenting a method for reducing the dimension of a large-scale network, while keeping the complete region of stable synchronization unchanged. To this aim, the first and last non-zero eigenvalues of the Laplacian matrix of a large network are preserved using the eigen-decomposition method and, Gram-Schmidt orthogonalization. The method is only applicable to undirected networks and the result is a weighted undirected network with smaller size. The reduction method is studied in a large-scale a small-world network of Sprott-B oscillators. The results show that the trend of the synchronization error is well maintained after node reduction for different coupling schemes.

Introduction. – The study of structural and dynamical features of real-world networks is facilitated using complex networks in different fields such as biology [1,2], neuroscience [3,4], ecology [5,6], and social science [7,8]. Synchronization is an important topic in complex networks [9–11]. Different types of synchronization have been found there, including complete [12], phase [13], cluster [14–16], explosive [17], and lag synchronization [18]. These synchronized states can emerge as the effect of the static or time-varying interactions in either attractive or repulsive couplings [19]. Moreover, enormous effort has been devoted to the controllability and observability of synchronized complex networks [20], improving the synchronizability [21, 22] and robustness of synchronization [23].

Most real-world systems can be better modeled by complex networks or even wih considering higher-order interactions [24]. These models may contain many nodes, making their analysis difficult and costly. Therefore, any efficient reduction of the size is of interest. One of the basic methods to decrease network size is graph partitioning. Various criteria exist whose persistence has been considered in reducing the network nodes. For instance, authors in [25] seek to keep some physical properties of the network after node reduction. Graph partitioning methods are mostly considered as non-deterministic polynomial-time problems [26], which cannot be solved in polynomial time. Therefore, researchers have tried to find other methods to reduce the network size. For example, Bona et al. [27] proposed a reduced model for the public transportation complex network with a long sequence of 2-degree nodes and some hubs. Despite removing 2-degree nodes, the reduced network has the same topological characteristics and skeleton as the original one. Besides, it was shown that this reduction increases the network cluster coefficient and the average degree while decreasing the path length.

Recently, different methods such as Spectral Coarse-Graining [28] and a Search Algorithm to Dimension Reduction [29] have been proposed. These algorithms decrease the dimension of the Laplacian matrix of the graph, while preserving some specific features of the parent network to keep synchronization. Whereas Spectral Coarse-Graining [28] iteratively reduces the dimension by merging the nodes, the Search Algorithm [29] can effectively reduce the number of nodes through a fast search. Another systematic approach for size reduction has been taken into account recently. In 2020, Thibeault et al. developed the Dynamics Approximate Reduction Technique to simplify a complex network [30]. Their method, which was based on spectral graph theory, enabled the prediction of the synchronization regimes of phase oscillators in large-scale networks by using dominant eigenvectors features. In this method, the reduced network size is not arbitrary and depends on the number of the network's communities. In [31], the authors have reduced the dimension of a non-locally coupled network by projecting the network dynamics onto the subspace that corresponds to the unstable eigenvalues of the linear part of the network.

In this paper, we introduce a novel approach to reduce the size of a complex undirected network with preserving its synchronization pattern. The key point for maintaining the synchronization stability of a network is to keep the eigenvalues of the Laplacian matrix that affect the synchronization within the master stability function approach. To this end, the eigen-decomposition and the Gram-Schmidt methods are utilized, and a smaller adjacency matrix which is weighted, is obtained.

The paper is organized as follows: First, the dimension reduction method is described in Section 2 in detail. Then, a large-scale network of chaotic Sprott-B systems is analyzed, and the preservation of synchronization pattern after reduction is checked. The results are presented in Section 3. Finally, the conclusions of the paper are given in Section 4.

Dimension reduction method. – This section describes the method used to reduce the dimension of a large undirected network to a smaller one. The aim is to preserve the synchronization pattern of the large-scale network after dimension reduction. It has been shown that the stability of synchronization in networks relies on the coupling topology [32]. According to the master stability function method [33], the region of stable synchronization depends on the eigenvalues of the connectivity matrix of the graph. Here, the reduction method is based on obtaining a reduced connectivity matrix with desired eigenvalues which are those involved in determining the synchronization stability region. The eigen-decomposition factorization is used for finding this reduced connectivity matrix.

Master stability function. The master stability function (MSF) [33] is a method for finding the local stability of synchronization. The description of this approach is given in the following.
It is supposed that N identical oscillators with the individual dynamics of $F(.)$ are linearly coupled by the overall coupling strength d through a Laplacian connection matrix G. For the oscillator i, one can write

$$\dot{X}_i = F\left(X_i\right) - d\sum_{j=1}^{N} G_{ij} H\left(X_j\right), \quad i = 1, 2, \ldots, N \tag{1}$$

where H indicates the coupling function. When all oscillators lie in the synchronization manifold, i.e., $X_1 = X_2 = \ldots = X_N = X_s$, the linearization of Eq. (1) around the synchronized solution X_s is defined as the variational equation and can be written as

$$\dot{\eta_l} = \left[DF\left(X_s\right) - \alpha_l DH\left(X_s\right)\right]\eta_l, \qquad l = 1, 2, \ldots, N \tag{2}$$

in which $\alpha_l = d\lambda_l$, where λ_l is the l^{th} eigenvalue of the matrix G. Also, DH and DF are the Jacobian matrixes of H and F, respectively. The variational equation (Eq. (2)) determines the stability of synchronization, which can be found by calculating its maximum Lyapunov exponent. The maximum Lyapunov exponent (Λ) of Eq. (2) as a function of $\alpha = d\lambda$ is known as the master stability function (MSF). Considering a connected and undirected network, the first eigenvalue of G is zero ($\lambda_1 = 0$), which is along the synchronization manifold. The other eigenvalues are sorted assendingly $\lambda_2 \leq \lambda_3 \leq \ldots \leq \lambda_N$. When $\Lambda < 0$ for all eigenvalues λ_i, $i = 2, \ldots, N$ of the Laplacian matrix, all the nodes of the network oscillate in complete synchrony.

Huang et al. [34] proposed a general scheme for categorizing the MSFs and introduced four classes. The classification is based on the number of zero-crossing points of the master stability function curve versus α, such that Γ_k represents a class in which $\Lambda(\alpha)$ crosses the zero k times. In case the synchronization cannot be reached for any α value, the master stability function has no zero-crossing point and is classified as Γ_0 (Fig. 1a). The master stability function with only one zero-crossing point, $\alpha_{\min}$, is known as class Γ_1, which is shown in Fig. 1b. Sorting the eigenvalues of the Laplacian matrix (G) in ascending order (i.e., $\lambda_1 = 0$), the synchronization manifold of this class is stable if

$$\alpha_{\min} < d\lambda_2 \leq d\lambda_3 \leq \ldots \leq d\lambda_N \tag{3}$$

holds. Hence, choosing the coupling strength as $d > \frac{\alpha_{\min}}{\lambda_2}$ ensures the stability of the synchronization manifold. In other words, the synchronization region, which is unbounded depends only on λ_2. In class Γ_2 (Fig. 1c), the master stability function versus α has two zero-crossing points, $\alpha_{\min}$ and $\alpha_{\max}$, where the region $\alpha_{\min} < \alpha < \alpha_{\max}$ is the stability region ($\Lambda < 0$). Therefore, an upper bound of the eigenvalues is also required for the stability region. In this case, the synchronization is stable if

$$\alpha_{\min} < d\lambda_2 \leq d\lambda_3 \leq \ldots \leq d\lambda_N < \alpha_{\max} \tag{4}$$

Consequently, synchronization can be achieved for $\frac{\alpha_{\min}}{\lambda_2} < d < \frac{\alpha_{\max}}{\lambda_N}$. By taking $R \equiv \frac{\lambda_N}{\lambda_2}$ as an eigenratio, the synchronization can occur if $R < \frac{\alpha_{\max}}{\alpha_{\min}}$. Thus, in this class,

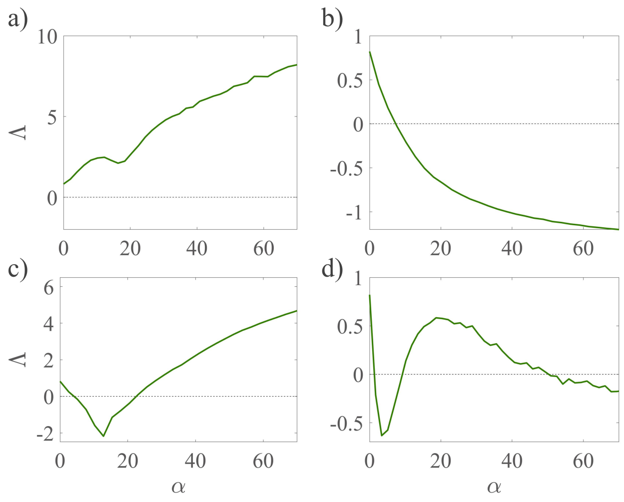

Fig. 1: Different classes of master stability function. **a)** Class Γ_0 with no zero-crossing point, **b)** class Γ_1 with only one zero-crossing point, **c)** class Γ_2 with two zero-crossing points, and **d)** class Γ_3 with three zero-crossing.

the stability region of synchronization depends only on the value of R. Barahona and Pecora [35] investigated the stability of synchronization in small-world networks by using the concept of the first-non-zero and maximum eigenvalues of the Laplacian matrix.

Finally, the fourth class belongs to the master stability function with more than two zero-crossing points; as an example, class Γ_3 with three zero-crossing is illustrated in Fig. 1d. For these systems, the synchronization can be achieved if all $d\lambda_i$ reside in the $\Lambda < 0$ regions. Since this class is more complex and case-dependent, we ignore it in this study.

According to the above definitions of the master stability function classifications, the synchronization region is only affected by λ_2 and λ_N. In fact, two networks have the same synchronization region if they have the same λ_2 and λ_N. Based on this concept, a reduced network can have the same synchronization pattern as the original network by choosing its λ_2 and $\lambda_{\max}$ the same as the original network. To find the connectivity matrix with defined eigenvalues, the eigen-decomposition approach can be used which is explained in the next subsection.

Eigen-decomposition and Gram-Schmidt orthogonalization of Laplacian matrix. Consider λ_i , $i = 1, 2, \ldots, N$ and λ'_i, $i = 1, 2, \ldots, n$ as the i^{th} eigenvalue of the original and reduced Laplacian matrix, respectively, and R and R' as their eigenratio as well. To have the same synchronization pattern, we must keep $\lambda_2 \cong \lambda'_2$ and also $R \cong R'$, leading to $\lambda_N \cong \lambda'_n$. To determine Laplacian matrix of the reduced network with desired eigenvalues, the eigen-decomposition factorization can be utilized. According to this factorization, any positive semidefinite matrix, e.g., A, can be factorized as

$$A = QDQ^{-1} \tag{5}$$

in which D is a diagonal matrix whose diagonal elements are the eigenvalues of A, and the corresponding eigenvectors lie in the columns of Q. Therefore, by considering D as the matrix of eigenvalues of the reduced matrix $(n \times n)$ and finding an appropriate eigenvector matrix (Q), the Laplacian matrix $A_{n\times n}$ can be computed using Eq. (5). Since the matrix A is assumed symmetric, we can write,

$$A = A^T = \left(QDQ^{-1}\right)^T = \left(Q^{-1}\right)^T DQ^T \tag{6}$$

leading to $Q^{-1} = Q^T$, where T denotes the transposed matrix. Therefore, Q must be an orthogonal matrix. To form an orthogonal basis, the Gram-Schmidt process can be used [see Appendix for more details]. Since the first eigenvalue of A is zero, its corresponding eigenvector must be chosen as $v_1 = [1, 1, \ldots, 1]_{1\times n}{}^T$ for the Gram-Schmidt process. Selecting the other independent basis vectors is arbitrary. Then, using the orthogonal basis vectors, $Q_{n\times n}$ can be obtained.

In order to determine $D_{n\times n}$, n eigenvalues in the ascending order are needed, where three of them are known: $\lambda'_1 = 0$, $\lambda'_2 = \lambda_2$, and $\lambda'_n = \lambda_N$. The rest of the needed eigenvalues ($n - 3$ eigenvalues) are found by partitioning the $N - 3$ eigenvalues of the Laplacian matrix of the original network. Here, we use the k-means clustering algorithm. K-means is the most popular clustering method due to its simplicity (for more detail, see [36]). After obtaining an orthogonal matrix Q, and a diagonal matrix D, a Laplacian matrix A with the desired dimension and eigenvalues can be found by using Eq. (5). It should be noted that the obtained matrix is weighted. The described method for obtaining the reduced connectivity matrix A is presented in Fig. 2.

Simulation results. – In this section, we apply the proposed method to reduce a high-dimensional Watts-Strogatz small-world network with $N = 500$ nodes and 10^5 links. It is assumed that the individual dynamics of the node obey the chaotic Sprott-B equations [37]:

$$\begin{cases} \dot{x} &= yz \\ \dot{y} &= x - y \\ \dot{z} &= 1 - xy \end{cases} \tag{7}$$

The size of the reduced network is assumed as $n = 100$ here. We consider different coupling functions to investigate different synchronization patterns. For the original network, we have $\lambda_2 = 339.47$ and $\lambda_N = 449.80$. Thus, we keep these eigenvalues and obtain the other $n - 3$ eigenvalues by classifying $N - 3$ eigenvalues of the original network. So, the matrix D is found. Next, the eigen-decomposition factorization and Gram-Schmidt orthogonalization are employed, and an orthogonal matrix of eigenvectors is obtained (Q). Finally, a zero-row sum, symmetry Laplacian matrix of size $n = 100$ with desired eigenvalues is found using Eq. (5). The values of the two most essential eigenvalues and eigenratio used in this example are represented in Table 1. It can be seen that

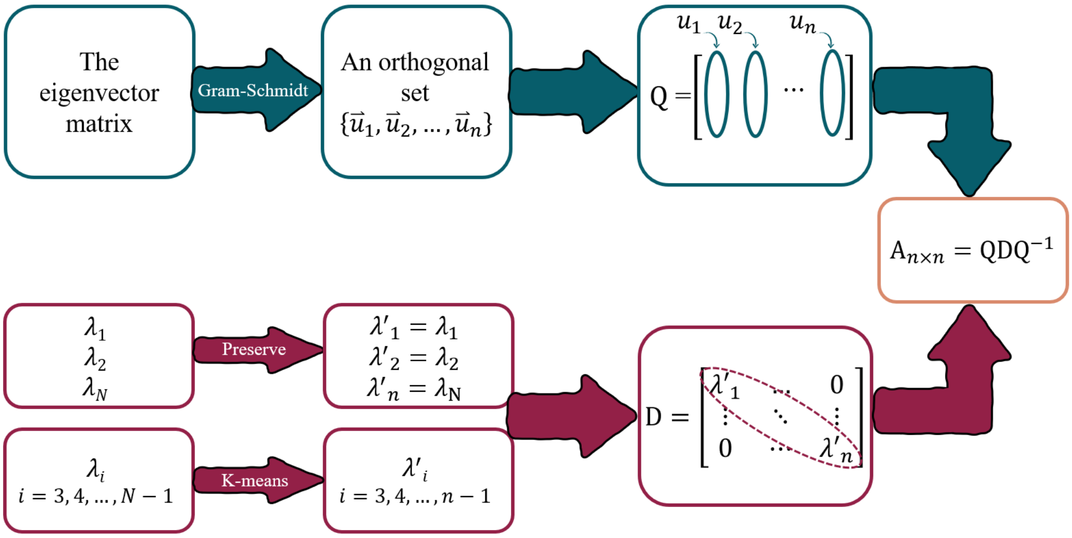

Fig. 2: The schematic of the proposed method to reduce an N-dimensional network to n-dimensional one ($N > n$) using eigen-decomposition factorization and Gram-Schmidt orthogonalization.

Table 1: Two eigenvalues and eigenratios of the reduced network and its parent.

	Original network	Reduced network
λ_2	339.47	339.50
$\lambda_{\max}$	449.80	449.80
R	1.32	1.32

the eigenvalues of the reduced and original networks are approximately equal.

For more investigation, three couplings with different MSF classes are considered. In Fig. 3, the master stability functions versus α are plotted. Three different couplings $y \to x$, $x \to y$, and $x \to z$ are considered. The notation, e.g., $x \to z$, means that the coupling which is defined on x state variables is added to z state variables. According to the eigenvalues presented in Table 1, the stability regions in $y \to x$ coupling are $d > 0.003069$ and $d > 0.003081$ for the original and reduced networks, respectively. For $x \to y$ coupling, the stability regions of the original and reduced networks are $0.002957 < d < 0.0031030$ and $0.002962 < d < 0.0031023$, respectively.

Next, the networks are solved numerically, and the synchronization error is calculated using Eq. 8.

$$Err = \frac{1}{T(N-1)} \lim_{T\to\infty} \int_0^T \sum_{k=2}^{N} \sqrt{(x_1 - x_k)^2 + (y_1 - y_k)^2 + (z_1 - z_k)^2}\, \mathrm{d}t \tag{8}$$

The synchronization errors for both networks and each coupling scheme are illustrated in Fig. 4. The upper and lower panels represent the errors of the parent and reduced networks, respectively. It can be observed that the synchronization regions, i.e., the region of coupling strength (d) with zero error, are the same for both networks. Moreover, the synchronization errors have similar trends in the original and reduced networks.

To better compare the synchronization behavior of both networks, time series, spatiotemporal patterns, and time snapshots are presented in Figs. 5-8 for synchronous and asynchronous states for master stability function of class Γ_1 and class Γ_2. Figure 5 illustrates the patterns of both networks for $d = 3.7 \times 10^{-3}$ which is in the synchronization regime under $y \to x$ coupling. Also, the results for $d = 2.7 \times 10^{-3}$ in which the oscillators of networks under $y \to x$ coupling are asynchronous, are shown in Fig. 6. Moreover, the networks have the same behavior for class Γ_2 ($x \to y$ coupling). In Fig. 7 and Fig. 8, the synchronous and asynchronous behavior of both networks is represented by considering $d = 3.0 \times 10^{-3}$ and $d = 3.2 \times 10^{-3}$, respectively. It can be observed that the networks have similar synchronous and asynchronous patterns.

Conclusion. – Large-scale complex networks are important models for describing various real-world networks. However, their high dimensionality often gives rise to high computational costs for analysis, leading to be time-consuming. Hence, reducing the dimension of these networks is essential. On the other hand, synchronization is a significant phenomenon in complex networks. Therefore, it is desired not to disturb the synchronization pattern during dimension reduction. This study addressed this issue by decreasing the size of the Laplacian matrix of a large-scale network using the eigen-decomposition method and the Gram-Schmidt orthogonalization process. The original network is considered to be undirected; therefore, the eigenvalues of the Laplacian matrix are real. To construct a network with eigen-decomposition approach, firstly, the eigenvalues of the reduced Laplacian matrix

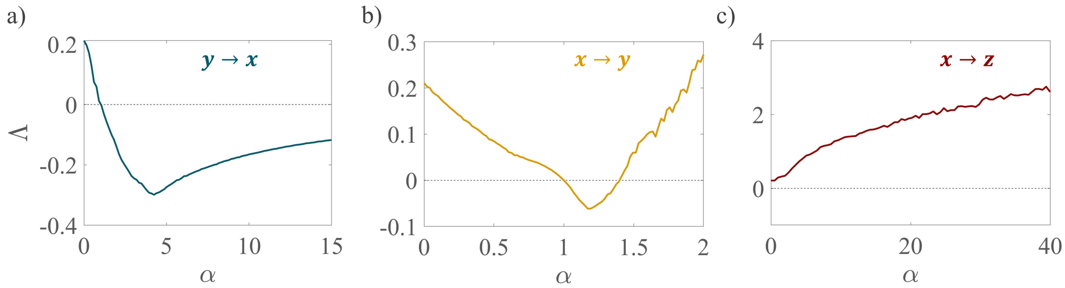

Fig. 3: The master stability function versus α for Sprott-B chaotic system (Eq. (7)) under three different couplings: **a)** $y \to x$ (class Γ_1), **b)** $x \to y$ (class Γ_2), and **c)** $x \to z$ (class Γ_0). Coupled Sprott-B systems represent different synchronization patterns according to the coupling scheme.

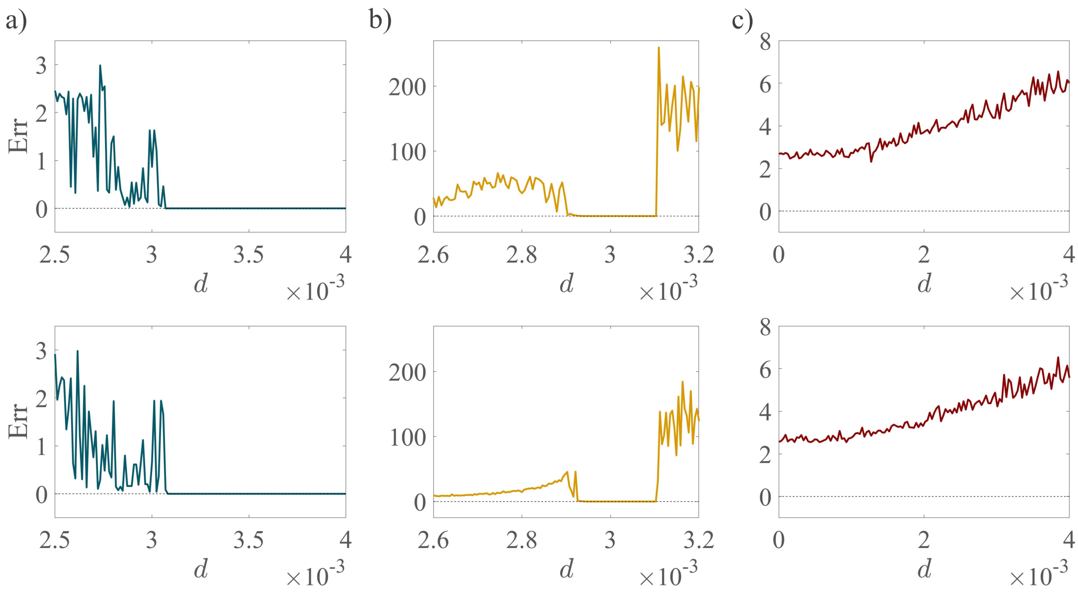

Fig. 4: The synchronization errors of coupled Sprott-B systems for the original (upper plots) and reduced (lower plots) networks as a function of coupling strength d. The coupling is on **a)** class Γ_1 ($y \to x$), **b)** class Γ_2 ($x \to y$), and **c)** class Γ_0 ($x \to z$). The synchronization region and the trend of error are similar for both networks in each class.

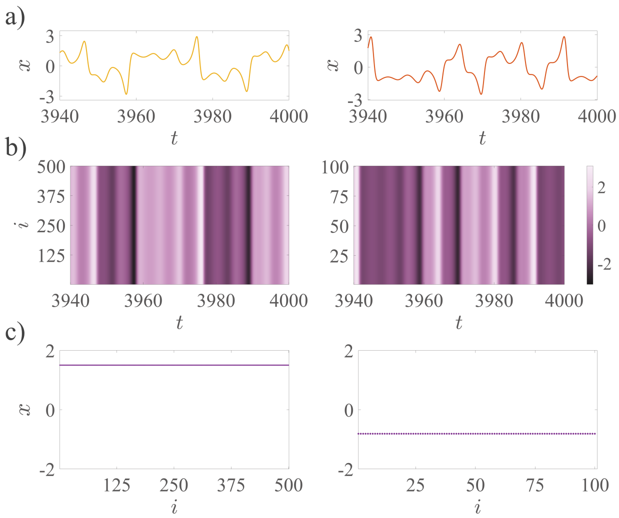

Fig. 5: **a)** Time series, **b)** spatiotemporal pattern, and **c)** time snapshot at $t = 4000$ for $y \to x$ coupling which is class Γ_1. The left and right panels are the results of the original network ($N = 500$) and the reduced one ($n = 100$), respectively. The coupling strength is $d = 3.7 \times 10^{-3}$, in which all oscillators lie in the synchronous manifold. The oscillations of both original and reduced networks are synchronous in this case.

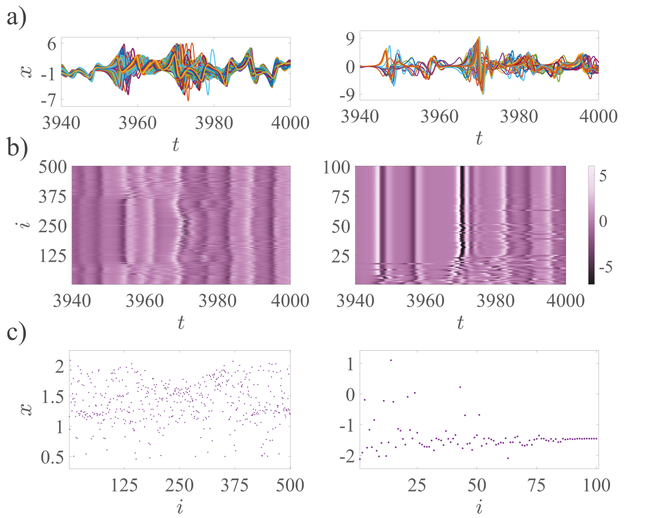

Fig. 6: **a)** Time series, **b)** spatiotemporal pattern, and **c)** time snapshot at $t = 4000$ for $y \to x$ coupling which is class Γ_1. The coupling strength is $d = 2.7 \times 10^{-3}$, that leads to asynchronous oscillations in the original (left panel) and the reduced networks (right panel). This case exhibits asynchronous oscillations in both networks.

must be defined. According to the master stability function, the region of stable synchronization depends on the minimum and maximum non-zero eigenvalues. Thus, we kept them the same as the original network and selected the other eigenvalues by classifying the original eigenvalues. Then, the matrix of eigenvectors was obtained by the Gram-Schmidt orthogonalization process. Finally, using the eigenvalues and eigenvectors, a weighted reduced Laplacian matrix was obtained. The method was applied on a 500-node small-world network of Sprott-B systems. The results were validated via synchronization error, time series, spatiotemporal patterns, and snapshots of both networks for different coupling functions in the synchronous and asynchronous states. Our findings indicate that the number of nodes of any complex network can be decreased regardless of network topology and node dynamics with preserving the synchronization stability region.

Conflict of interest. – The authors declare that they have no conflict of interest.

APPENDIX: the Gram-Schmidt process. – Suppose the arbitrary set $\{\overrightarrow{v}_1, \overrightarrow{v}_2, \ldots, \overrightarrow{v}_k\}$ as the basis for a given set V, whose vectors are linearly independent. The Gram-Schmidt process can generate an orthogonal basis for V. The vectors $\{\overrightarrow{u}_1, \overrightarrow{u}_2, \ldots, \overrightarrow{u}_k\}$ are said to be orthogonal if and only if the inner product of any two different vectors of them is equal to zero, i.e., $\langle \overrightarrow{u}_i, \overrightarrow{u}_j \rangle = 0 \ \forall \ i \neq j$. This set of new vectors can be constructed as follows:

$$\begin{cases} \overrightarrow{u}_1 &= \overrightarrow{v}_1 \\ \overrightarrow{u}_2 &= \overrightarrow{v}_2 - \frac{\langle \overrightarrow{v}_2, \overrightarrow{u}_1 \rangle}{\langle \overrightarrow{u}_1, \overrightarrow{u}_1 \rangle} \overrightarrow{u}_1 \\ \overrightarrow{u}_3 &= \overrightarrow{v}_3 - \frac{\langle \overrightarrow{v}_3, \overrightarrow{u}_1 \rangle}{\langle \overrightarrow{u}_1, \overrightarrow{u}_1 \rangle} \overrightarrow{u}_1 - \frac{\langle \overrightarrow{v}_3, \overrightarrow{u}_2 \rangle}{\langle \overrightarrow{u}_2, \overrightarrow{u}_2 \rangle} \overrightarrow{u}_2 \\ \vdots & \\ \overrightarrow{u}_k &= \overrightarrow{v}_k - \sum_{p=1}^{k-1} \frac{\langle \overrightarrow{v}_k, \overrightarrow{u}_p \rangle}{\langle \overrightarrow{u}_p, \overrightarrow{u}_p \rangle} \overrightarrow{u}_p \end{cases}$$

where $\langle . \rangle$ denotes the inner product.

REFERENCES

[1] Ivanov P. C., *Front. Netw. Physiol.*, (2021) 711778.
[2] Gosak M., Milojević M., Duh M., Skok K. and Perc M., *Phys. Life Rev.*, **41** (2022) 1.
[3] Rakshit S., Majhi S., Kurths J. and Ghosh D., *Chaos*, **31** (2021) 073129.
[4] Chouzouris T., Omelchenko I., Zakharova A., Hlinka J., Jiruska P. and Schöll E., *Chaos*, **28** (2018) 045112.
[5] Kundu S., Majhi S. and Ghosh D., *Chaos*, **31** (2021) 033154.
[6] Chowdhury S. N., Kundu S., Perc M. and Ghosh D., *Proc. R. Soc. A*, **477** (2021) 20210397.
[7] Kumar A., Chowdhary S., Capraro V. and Perc M., *Phys. Rev. E*, **104** (2021) 054308.
[8] Han S. and Kim B. J., *Physica A*, **387** (2008) 5946.
[9] Boccaletti S., Kurths J., Osipov G., Valladares D. L. and Zhou C., *Phys. Rep.*, **366** (2002) 1.
[10] Pikovsky A., Rosenblum M. and Kurths J., *Am. J. Phys.*, **70** (2001) .
[11] Hong H., Choi M. Y. and Kim B. J., *Phys. Rev. E*, **65** (2002) 026139.

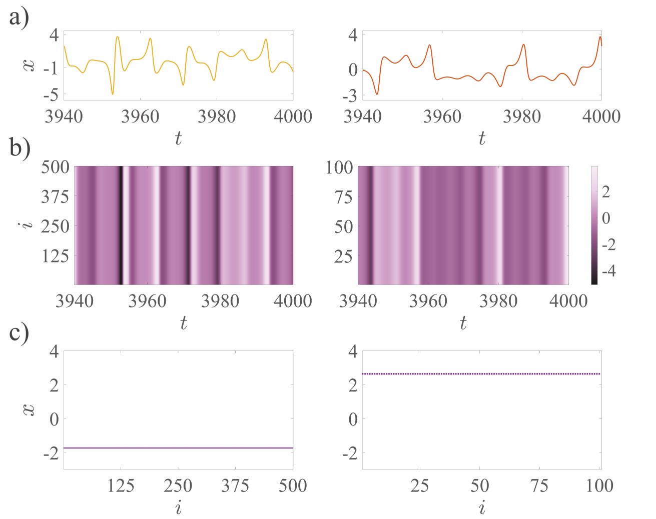

Fig. 7: **a)** Time series, **b)** spatiotemporal pattern, and **c)** time snapshot at $t = 4000$ for $x \to y$ coupling which is class Γ_2 for the original (left panel) and the reduced networks (right panel) at $d = 3.0 \times 10^{-3}$. Synchronized oscillations are observed in both networks.

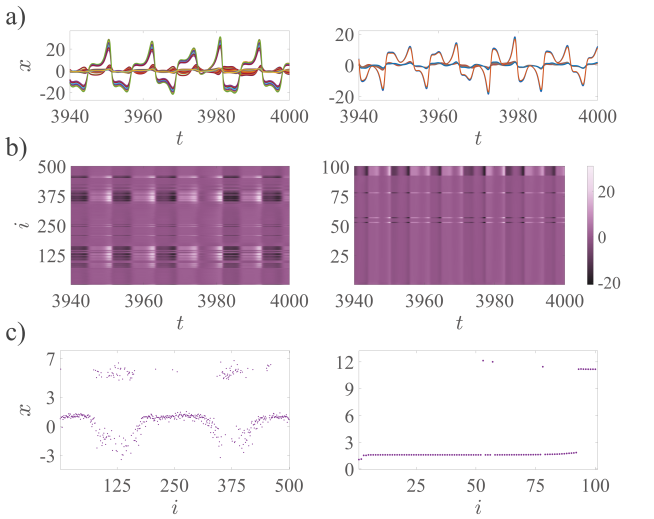

Fig. 8: **a)** Time series, **b)** spatiotemporal pattern, and **c)** the last time snapshot at $t = 4000$ for $x \to y$ coupling, which is class Γ_2, with $d = 3.2 \times 10^{-3}$. Asynchronous oscillations are observed in both the left panel (the original network) and the right panel (the reduced network). It appears that in this case both networks oscillate asynchronously.

[12] Wang P., Wen G., Yu X., Yu W. and Huang T., *IEEE Trans. Circuits Syst. I Regul. Pap.*, **66** (2018) 1141.

[13] Pikovsky A., Rosenblum M. and Kurths J., *Int. J. Bifurcation Chaos*, **10** (2000) 2291.

[14] Panahi S., Klickstein I. and Sorrentino F., *Chaos*, **31** (2021) 111102.

[15] Sorrentino F. and Ott E., *Phys. Rev. E*, **76** (2007) 056114.

[16] Dahms T., Lehnert J. and Schöll E., *Phys. Rev. E*, **86** (2012) 016202.

[17] Jalan S., Kumar A. and Leyva I., *Chaos*, **29** (2019) 041102.

[18] Rosenblum M. G., Pikovsky A. S. and Kurths J., *Phys. Rev. Lett.*, **78** (1997) 4193.

[19] Sar G. K., Chowdhury S. N., Perc M. and Ghosh D., *New J. Phys.*, **24** (2022) 043004.

[20] Sorrentino F., Di Bernardo M., Garofalo F. and Chen G., *Phys. Rev. E*, **75** (2007) 046103.

[21] Rakshit S., Bera B. K., Kurths J. and Ghosh D., *Proc. R. Soc. A*, **475** (2019) 20190460.

[22] Hong H., Kim B. J., Choi M. Y. and Park H., *Phys. Rev. E*, **69** (2004) 067105.

[23] Parastvand H., Chapman A., Bass O. and Lachowicz S., *Control Eng. Pract.*, **108** (2021) 104705.

[24] Majhi S., Perc M. and Ghosh D., *J. R. Soc. Interface.*, **19** (2022) 20220043.

[25] Martin N., Frasca P. and Canudas-de Wit C., *IEEE Trans. Network Sci. Eng.*, **6** (2018) 711.

[26] Bui T. N. and Jones C., *Inf. Process. Lett.*, **42** (1992) 153.

[27] De Bona A. A., de Oliveira Rosa M., Fonseca K. V. O. and Lüders R., *Physica A*, **567** (2021) 125715.

[28] Zeng L., Jia Z. and Wang Y., *Commun. Netw*, **10** (2018) 93.

[29] Naseri N., Parastesh F., Karami M. and Ghassemi F., *Eur. Phys. J. Spec. Top.*, (2022) In Press.

[30] Thibeault V., St-Onge G., Dubé L. J. and Desrosiers P., *Phys. Rev. Res.*, **2** (2020) 043215.

[31] Tumash L., Panteley E., Zakharova A. and Schöll E., *Eur. Phys. J. B*, **92** (2019) 100.

[32] Flunkert V., Yanchuk S., Dahms T. and Schöll E., *Phys. Rev. Lett.*, **105** (2010) 254101.

[33] Pecora L. M. and Carroll T. L., *Phys. Rev. Lett.*, **80** (1998) 2109.

[34] Huang L., Chen Q., Lai Y. C. and Pecora L. M., *Phys. Rev. E*, **80** (2009) 036204.

[35] Barahona M. and Pecora L. M., *Phys. Rev. Lett.*, **89** (2002) 054101.

[36] Jain A. K. and Dubes R. C., *Algorithms for clustering data* (Prentice-Hall, Inc.) 1988.

[37] Sprott J. C., *Phys. Rev. E*, **50** (1994) R647.